Molecular Vision 2014; 20:1643-1659 <http://www.molvis.org/molvis/v20/1643>
Received 10 September 2014 | Accepted 6 December 2014 | Published 9 December 2014

© 2014 Molecular Vision

Scleral gene expression during recovery from myopia compared with expression during myopia development in tree shrew

Lin Guo, Michael R. Frost, John T. Siegwart Jr., Thomas T. Norton

Department of Vision Sciences, School of Optometry, University of Alabama at Birmingham, Birmingham, AL

Purpose: During postnatal refractive development, the sclera receives retinally generated signals that regulate its biochemical properties. Hyperopic refractive error causes the retina to produce "GO" signals that, through the direct emmetropization pathway, cause scleral remodeling that increases the axial elongation rate of the eye, reducing the hyperopia. Myopia causes the retina to generate "STOP" signals that produce scleral remodeling, slowing the axial elongation rate and reducing the myopia. Our aim was to compare the pattern of gene expression produced in the sclera by the STOP signals with the GO gene expression signature we described previously.

Methods: The GO gene expression signature was produced by monocular –5 diopter (D) lens wear for 2 days (ML-2) or 4 days (ML-4); an additional "STAY" condition was examined after eyes had fully compensated for a –5 D lens after 11 days of lens wear (ML-11). After 11 days of −5 D lens wear had produced full refractive compensation, gene expression in the STOP condition was examined during recovery (without the lens) for 2 days (REC-2) or 4 days (REC-4). The untreated contralateral eyes served as a control in all groups. Two age-matched normal groups provided a comparison with the treated groups. Quantitative real-time PCR was used to measure mRNA levels for 55 candidate genes.

Results: The STAY group compensated fully for the lens (treated eye versus control eye, –5.1±0.2 D). Wearing the lens, the hyperopic signal for elongation had dissipated (–0.3±0.3 D). In the STOP groups, the refraction in the recovering eyes became less myopic relative to the control eyes (REC-2, +1.3±0.3 D; REC-4, +2.6±0.4 D). In the STAY group, three genes showed significant downregulation. However, many genes that were significantly altered in GO showed smaller, nonsignificant, expression differences in the same direction in STAY, suggesting the gene expression signature in STAY is a greatly weakened form of the GO signature. In the STOP groups, a different gene expression pattern was observed, characterized by mostly upregulation with larger fold differences after 4 days than after 2 days of recovery. Eleven of the 55 genes examined showed significant bidirectional GO/STOP regulation in the ML-2 and REC-2 groups, and 13 genes showed bidirectional regulation in the ML-4 and REC-4 groups. Eight of these genes (*NPR3*, *CAPNS1*, *NGEF*, *TGFB1*, *CTGF*, *NOV*, *TIMP1*, and *HS6ST1*) were bidirectionally regulated at both time points in the GO and STOP conditions. An additional 15 genes showed significant regulation in either GO or STOP conditions but not in both.

Conclusions: Many genes are involved in scleral remodeling and the control of axial length. The STOP (recovery) gene expression signature in the sclera involves some of the same genes, bidirectionally regulated, as the GO signature. However, other genes, regulated in GO, are not differentially regulated in STOP, and others show differential regulation only in STOP.

Refractive error occurs when there is a mismatch between the focal plane where images are in focus and the location of the retina, which is controlled by the axial length of the eye. When distant objects are in focus on the retina without accommodation, the eye is emmetropic. If the axial length (front of the cornea to the retina) is shorter than the focal plane, the eye is hyperopic. If the axial elongation of the globe moves the retina behind the focal plane, the eye becomes myopic. Myopia is the most prevalent type of refractive error worldwide, affecting 25–42% of the population in the US and in European countries [1-6]. In East Asia, the prevalence reaches as high as 85–96.5% [7-12]. Myopia is not only a refractive problem but also an important risk factor for blinding conditions, such as glaucoma, cataract, retinal detachment, choroidal degeneration, and other conditions [13-16]. Myopia prevalence also is increasing, forecasting an increase in these conditions over time [17]. Uncorrected myopia is surprisingly common worldwide and after cataracts is the leading cause of correctable visual impairment [18]. Thus, it is important to try to determine the causes of human myopia and in particular the mechanisms that regulate the axial length of the eye.

Studies of postnatal refractive development in both children and animal models (fish, chicks, monkeys, guinea pigs, tree shrews, and other species) have found that there is a visually guided emmetropization mechanism that uses visual cues to modulate the elongation of the globe so that the retina comes to be located at the focal plane [19-31]. The emmetropization mechanism can be stimulated to

Correspondence to: Thomas T. Norton, Department of Vision Sciences, 606 Worrell Building, University of Alabama at Birmingham, Birmingham, AL 35294-4390; Phone: (205) 934-6742; FAX (205) 934-5725; email: tnorton@uab.edu

produce increased axial elongation and myopia in animal models by placing a concave (minus-power) lens in front of an emmetropizing eye. This moves the focal plane away from the cornea, producing a hyperopic mismatch between the focal plane and the retina. In response, neurons in the retina generate what has been characterized as GO signals [32,33]. Over a period of a few days, the retina is moved to the shifted focal plane, restoring age-normal emmetropia [30,34,35]. Increased axial elongation can be detected in tree shrews after as little as 2 days of wearing a –5 diopter (D) lens [30]. After 11 days of continuous –5 D lens wear, the axial length of the eye has matched the new focal plane so the eye's refraction, while wearing the lens, matches that of the untreated fellow control eye [30]. Although at this point the refractive hyperopia that triggered the retinal GO signals has dissipated, the eye remains elongated as long as minus-lens wear is continued [30]. This has been referred to as a STAY condition [36].

When lens wear is discontinued after an eye has compensated refractively to the minus lens, the eye experiences myopia due to the elongated globe. The retina then produces STOP signals that slow the axial elongation rate of the eye below normal while the eye's optical power continues to move the focal plane away from the cornea, producing refractive recovery. Recovery continues until the axial length and the refractive state of the recovering eye match those of the control eye and of age-matched normal eyes [30,37].

These changes in the location of the retina are controlled by the sclera, which is an extracellular matrix (ECM). In mammals, the sclera is comprised primarily of layers (lamellae) of fibrillar type I collagen [38], along with many other components (e.g., proteoglycans, elastin, matricellular proteins) that are typically associated with fibrous connective tissue [39]. The retinally generated GO and STOP signals travel to the sclera through a "direct emmetropization pathway" that involves a signaling cascade through the RPE and the choroid that produces biochemical and biomechanical changes in the sclera. These control the viscoelasticity of the sclera and in turn the axial elongation rate [40].

To understand how scleral remodeling is accomplished, we have examined gene expression and protein level changes in the sclera [41-44]. Recently, we expanded our studies to examine changes in mRNA levels for 55 candidate genes in GO conditions. We found that three different stimulus conditions that produce a GO situation (minus-lens wear, form deprivation, and dark treatment) all produce similar patterns of gene expression that we described as a scleral GO signature [45]. In the present study, we compare that GO signature with the gene expression for the same 55 genes in STAY and STOP conditions.

Our objective was to learn, using this enlarged group of candidate genes examined at adjusted time points, whether the remodeling that slows axial elongation (STOP) involves altered expression in the same genes whose expression is altered in the remodeling that increases axial elongation (GO). In particular, are there genes that show changes in expression in a bidirectional manner, such as downregulation in STOP and upregulation in GO? To compare the early alterations in gene expression with those occurring later, we examined groups after 2 and 4 days of recovery to compare with groups that we had examined after 2 and 4 days of minus-lens wear. Further, because a recent study found evidence for a STAY gene expression signature in tree shrew choroid in animals that had fully compensated for a minus lens but were still wearing the lens [36], we examined scleral gene expression in a group that also had compensated fully for the lens after 11 days of treatment.

METHODS

Experimental groups: The methods used in this study were similar to those employed in previous studies from this laboratory [36,45]. We used juvenile tree shrews (*Tupaia glis belangeri*) that were raised in our breeding colony by their mothers on a 14 h:10 h light-dark cycle. All procedures complied with the ARVO Statement for the Use of Animals in Ophthalmic and Visual Research and were approved by the Institutional Animal Care and Use Committee of the University of Alabama at Birmingham. The first day both eyes are open, which occurs about 3 weeks after birth, was considered to be the first day of visual experience (DVE). Experimental groups were balanced to include both males and females and avoided pups from the same parents wherever possible. Right and left eyes were balanced as treated and control eyes in each group.

Seven groups of animals (n=7 per group) were used in this study (Figure 1). The two minus-lens wear groups (ML-2 and ML-4; GO) reported previously [45] wore a monocular –5 D (spherical power) lens for either 2 or 4 days, starting at 24±1 DVE. The gene expression in these animals is presented here to allow direct comparison of the STAY and STOP responses with the GO signature. A third minus-lens wear group (ML-11; STAY) wore a monocular −5 D lens for 11 days and fully compensated for the lens. At this point the refractive hyperopia that produced the retinal GO signal had dissipated and the eyes were emmetropic while wearing the lens. Two STOP groups began recovery at 35±1 DVE after 11 days of monocular minus-lens wear. They experienced

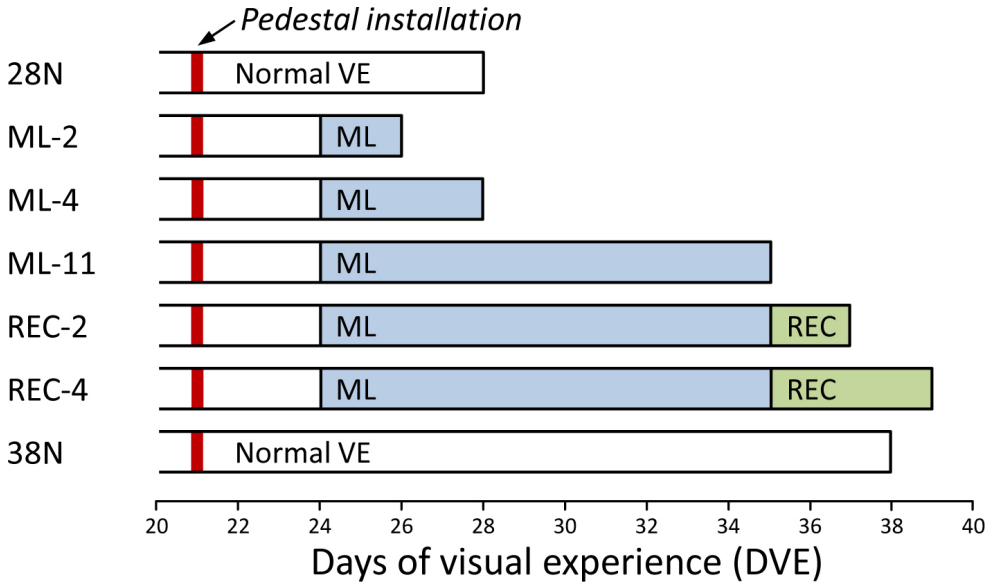

Figure 1. Experimental groups and duration of treatments. The red vertical bar indicates the point when a dental acrylic pedestal was installed under anesthesia. Filled regions indicate the type and duration of visual treatment. The right end of each bar indicates the time point when mRNA levels were measured. Abbreviations: VE represents visual experience, ML represents minus lens, REC represents recovery.

unrestricted vision for 2 (REC-2) or 4 (REC-4) days. In all ML and REC groups, the untreated fellow eye served as a control. Two age-matched normal groups were used, one at 28 DVE (28N; reported previously [45]) for comparison with the ML-2 and ML-4 groups, the other at 38 DVE (38N) for comparison with the ML-11, REC-2, and REC-4 groups.

In both the GO and STOP conditions, the 2-day treatment duration was used to examine gene expression soon after the start of treatment or recovery because a previous study found that after only 1 day, few changes in gene expression occurred in the sclera [43]. The 4-day duration was chosen to examine gene expression when the sclera would be undergoing maximal remodeling in both conditions [40].

Goggle installation: At 21±1 DVE, animals in all groups were anesthetized (17.5 mg ketamine, 1.2 mg xylazine injected intramuscularly; supplemented with 0.5–2.0% isoflurane as needed) in order for a dental acrylic pedestal to be attached to the skull [46] (Figure 1). After pedestal installation, all animals were placed in individual cages with standard colony fluorescent lighting, 100–300 lux on the floor of the cage. Three days later, in the ML and REC groups, a goggle frame holding a –5 D lens (12-mm diameter Poly(methyl methacrylate) (PMMA) contact lens; Conforma Contact Lenses, Norfolk, VA) was clipped to the pedestal, firmly holding the lens in front of the treated eye. The untreated contralateral control eye had unrestricted vision through an open goggle frame. Twice daily (approximately 9:30 AM and 4:30 PM), the goggles were briefly (<3 min) removed for lens cleaning under dim illumination while the animals were kept in a darkened nest box to minimize exposure to visual stimuli. The normal groups did not wear a goggle.

Refractive and axial measures: At the start and end of the treatments, non-cycloplegic refractive measures were taken in awake animals with a Nidek ARK-700A infrared autorefractor (Marco Ophthalmic, Jacksonville, FL) [47]. Measures were made at intermediate time points in some animals. Normal animals were measured just before euthanasia. Since atropine may interfere with retinoscleral signaling, cycloplegic refractive measures were omitted [48]. However, previous studies have shown that non-cycloplegic measures provide a valid estimate of the refractive state and of induced myopia in tree shrews [49,50]. All refractive values were corrected for the small eye artifact [51], previously shown to be approximately +4 D in tree shrews [47].

Ocular component dimensions were measured by A-scan ultrasound under anesthesia (15 MHz transducer focused at 20 mm, coupled with 0.9% saline-filled 14 mm Plexiglass standoff) at the time the pedestal was installed, as previously described [52], to ensure that experimental eyes did not differ significantly in axial length before treatment began. Post-treatment A-scan measures were avoided to eliminate any possibility that the anesthesia required for the A-scan procedure might alter gene expression. A Lenstar LS-900 optical biometer (Haag-Streit USA, Mason, OH) was used to make posttreatment axial component measures in the ML-2 group only. This instrument was placed into service after the other groups were completed and allowed measures to be quickly made in awake animals before euthanasia. Comparison of A-scan and Lenstar measures of the vitreous chamber in

animals in this laboratory showed that the axial differences measured with the Lenstar were similar to those measured with A-scan ultrasound (data not shown).

Tissue preparation: After completion of the final refractive measures, approximately 2–4 h into the light phase, animals were terminally anesthetized (17.5 mg ketamine and 1.2 mg xylazine, followed by 50 mg xylazine, intramuscular injection); both eyes were enucleated and placed into RNAlater solution (Life Technologies, Carlsbad, CA). Extraocular muscles, conjunctiva, and orbital fat were trimmed from the exterior surface of the eye, and the cornea was dissected away just behind the corneoscleral junction. After removing the lens, vitreous humor, and optic nerve head, both surfaces of the sclera were gently "scraped" to remove the retina, RPE, choroid, and any residual extraocular tissue before freezing the tissue in liquid nitrogen.

Gene expression analysis: Individual frozen scleras were pulverized to a fine powder in a chilled Teflon freezer mill (Sartorius Stedim, Bohemia, NY) from which total RNA was isolated using a RiboPure kit (Life Technologies) according to the manufacturer's instructions, with the addition of an on-filter DNase treatment. The purified RNA was quantified (NanoDrop Technologies, Wilmington, DE) with an average yield per sclera of 6.8±1.6 µg (mean ± standard deviation [SD]). RNA quality was confirmed by denaturing gel electrophoresis (RNA FlashGel; Lonza, Rockland, ME). cDNA was synthesized from 1 µg of total RNA in a final reaction volume of 20 µl using a Superscript III RT kit (Life Technologies) with minor modifications (2.5-µM anchored oligo (dT)20 primers and dithiothreitol [DTT] omitted). The resultant cDNA was diluted fivefold and stored at –20 °C until use.

Tree shrew-specific quantitative PCR (qPCR) primers were designed for 55 genes of interest (Table 1) and the reference gene RNA polymerase II (POLR2A) using Beacon Designer v7.7 (Premier Biosoft International, Palo Alto, CA). None of the treatment conditions affected the expression of the reference gene. Primer sequences, amplicon size, and efficiencies are listed in Appendix 1. All primers were designed to work under the same cycling conditions. All amplicons were located within the coding region and most spanned at least one intron; amplicon identity was verified by gel electrophoresis and sequencing.

Because there are no commercial gene arrays for tree shrews, we examined expression in 55 candidate genes. These included representatives of three major groupings: signaling, metallopeptidases and tissue inhibitors of metallopeptidases (TIMPs), and extracellular matrix (ECM) proteins. They were selected from genes that were found to change in previous studies of tree shrew sclera during minus-lens wear [43,53,54], along with additional genes whose expression seemed likely to change based on studies in other species and by a preliminary whole-transcriptome analysis of three of the ML-4 animals. While recognizing that this would not comprehensively identify all involved genes, the sample was large enough to fulfil the purpose of this study—to compare the expression of these representative genes in the GO, STAY, and STOP conditions.

Relative gene expression was measured by qPCR on a StepOnePlus Real-Time PCR System using Power SYBR Green PCR Master Mix (both, Life Technologies). Reactions were performed in triplicate in a 15-µl volume containing 300 nM of each primer and 0.4 µl of cDNA template. Cycling parameters were the same for all assays: initial denaturation at 95 °C for 10 min, followed by 40 cycles of 95 °C for 15 s, 62 °C for 60 s. Single gene-products were obtained for all reactions as assessed by melt curve analysis. Relative gene expression was calculated using the $^{\Delta\Delta}$Ct method [55] to first normalize the expression level of the target gene to that of the reference gene and then to compare the relative expression of the target gene for treated versus control eyes, treated versus normal eyes (mean of right and left eyes), and right versus left eyes of normal animals. The geometric group mean (for the seven biologic replicates) of these expression ratios was used to calculate the fold change in gene expression for each of the target genes.

Statistical analysis: One-way analysis of variance (ANOVA) (STATISTICA; Statsoft, Tulsa, OK) was used to compare control and normal eye refractive data across groups of animals; paired *t* tests were used to determine if significant myopia (treated eye versus control eye) or recovery had occurred. For gene expression data, paired *t* tests were used to assess treated eye versus control eye differences; unpaired *t* tests were used to test for gene expression differences between all independent groups. In all cases, $p<0.05$ was considered significant, and no adjustment was applied for a possible false discovery rate. Linear regressions between expression differences were made in SigmaPlot (Systat Software, San Jose, CA).

RESULTS

Refraction: As shown in Figure 2A, the refractive differences between right and left eyes of the two normal groups were negligible (mean±standard error of the mean [SEM] of the right-eye refraction – the left-eye refraction: 28N, 0.01±0.2 D; 38N, −0.02±0.2 D). As reported previously [45], the ML-2 treated eyes (Figure 2B) showed a small, statistically significant, myopic shift (−1.0±0.2 D) relative to the control eyes. The myopic shift in the ML-4 group was −2.8±0.3 D.

Table 1. Genes examined, divided into functional categories, with cellular location of the protein encoded by the gene.

Gene symbol	Protein name	Location
	Signaling − Cell surface	
ACVRL1	Activin A receptor 2-like 1	Cell surface
FGFR2	FGF receptor 2	Cell surface
NPR3	Atrial natriuretic peptide receptor 3	Cell surface
SDC2	Syndecan 2	Cell surface
TGFBR3	TGFβ receptor III	Cell surface
TRPV4	Transient receptor potential cation channel V4	Cell surface
UNC5B	Netrin receptor UNC5B	Cell surface
EFNA1	Ephrin A1	Cell surface
	Signaling − Cytoskeleton related	
ANXA1	Annexin A1	Cell surface
ANXA2	Annexin A2	Cell surface
CAPN2	Calpain 2	Cell surface
CAPNS1	Calpain small subunit 1	Cell surface
GJA1	Connexin 43	Cell surface
ACTA2	Smooth muscle actin	Intracellular
NGEF	Neuronal guanine nucleotide exchange factor	Intracellular
	Signaling − Transcription regulators	
HIF1A	Hypoxia-inducible factor 1α	Intracellular
RARB	Retinoic acid receptor β	Intracellular
RXRB	Retinoid X receptor β	Intracellular
VDR	Vitamin D receptor	Intracellular
	Signaling − Secreted	
ANGPTL7	Angiopoietin-related protein 7	Extracellular
IGF1	Insulin-like growth factor 1	Extracellular
IGF2	Insulin-like growth factor 2	Extracellular
IL18	Interleukin 18	Extracellular
PENK	Proenkephalin A	Extracellular
TGFB1	Transforming growth factor β1	Extracellular
TGFB2	Transforming growth factor β2	Extracellular
TGFBI	TGFβ-induced protein	Extracellular
	Signaling − Matricellular	
CTGF	Connective tissue growth factor	Extracellular

Molecular Vision 2014; 20:1643-1659 <http://www.molvis.org/molvis/v20/1643>

© 2014 Molecular Vision

Gene symbol	Protein name	Location
CYR61	Protein CYR61	Extracellular
FBLN1	Fibulin 1	Extracellular
NOV	Protein NOV homolog	Extracellular
SPARC	Secreted protein acidic and rich in cysteine	Extracellular
SPP1	Osteopontin	Extracellular
THBS1	Thrombospondin 1	Extracellular
THBS2	Thrombospondin 2	Extracellular
TNC	Tenascin C	Extracellular
WISP1	WNT1 inducible signaling pathway protein 1	Extracellular
	MPs / TIMPs	
ADAMTS5	ADAM metallopeptidase with thrombospondin motif, 5	Extracellular
MMP2	Matrix metallopeptidase 2	Extracellular
MMP14	Matrix metallopeptidase 14	Cell surface
TIMP1	TIMP metallopeptidase inhibitor 1	Extracellular
TIMP2	TIMP metallopeptidase inhibitor 2	Extracellular
TIMP3	TIMP metallopeptidase inhibitor 3	Extracellular

Molecular Vision 2014; 20:1643-1659 <http://www.molvis.org/molvis/v20/1643>

© 2014 Molecular Vision

The myopia in the ML-11 group was −5.1±0.2 D; measured with the lens in place, the treated eyes were slightly myopic (−0.3±0.3 D) compared with their fellow control eyes, and all treated eyes were within 1 D of the control eyes. Thus, the lens-induced hyperopia present at the start of lens wear had dissipated. After fully compensating for the minus lens, the REC-2 treated eyes became less myopic by 1.3±0.3 D (Figure 2C). The REC-4 group recovered by 2.6±0.4 D. The control eyes in the ML and REC groups did not differ significantly from the normal eyes in the 28N and 38N groups (one-way ANOVA, p=0.17).

Posttreatment ocular component dimensions of the eyes in the ML-2 group confirmed that the vitreous chamber of the treated eyes had elongated slightly relative to the control eyes by 0.016±0.004 mm [45]. Although the axial changes were not measured in the other groups, the results of previous studies of tree shrews [40-42,49,56-58] make it reasonable to assume that the myopic shifts after 4 days and 11 days of ML were due to an increase in vitreous chamber depth of approximately 0.060 to 0.075 mm and that the differences in the recovery groups were smaller than they had been after compensation to the minus lens.

Gene expression:

Normal animals—Figure 3 compares gene expression in the right and left eyes of the two groups of normal animals, measured at 28 DVE and 38 DVE. Fold differences (listed in Figure 4) were small without regard to sign (mean±SD, 1.11±0.08 in the 28N group and 1.12±0.15 in the 38N group). Only one of the genes in our sample at 28N, the alpha chain of type 1 collagen (*COL1A1*), was slightly, but significantly, higher in the right eyes (mean±SEM,1.17±0.05, p=0.0208). None of the genes in the 38N group differed significantly.

GO: 2-day and 4-day minus lens treatment: The fold differences in gene expression between the treated and control eyes in the GO groups (ML-2 and ML-4) are shown in Figure 5A,B; expression values are also listed in Figure 4. The

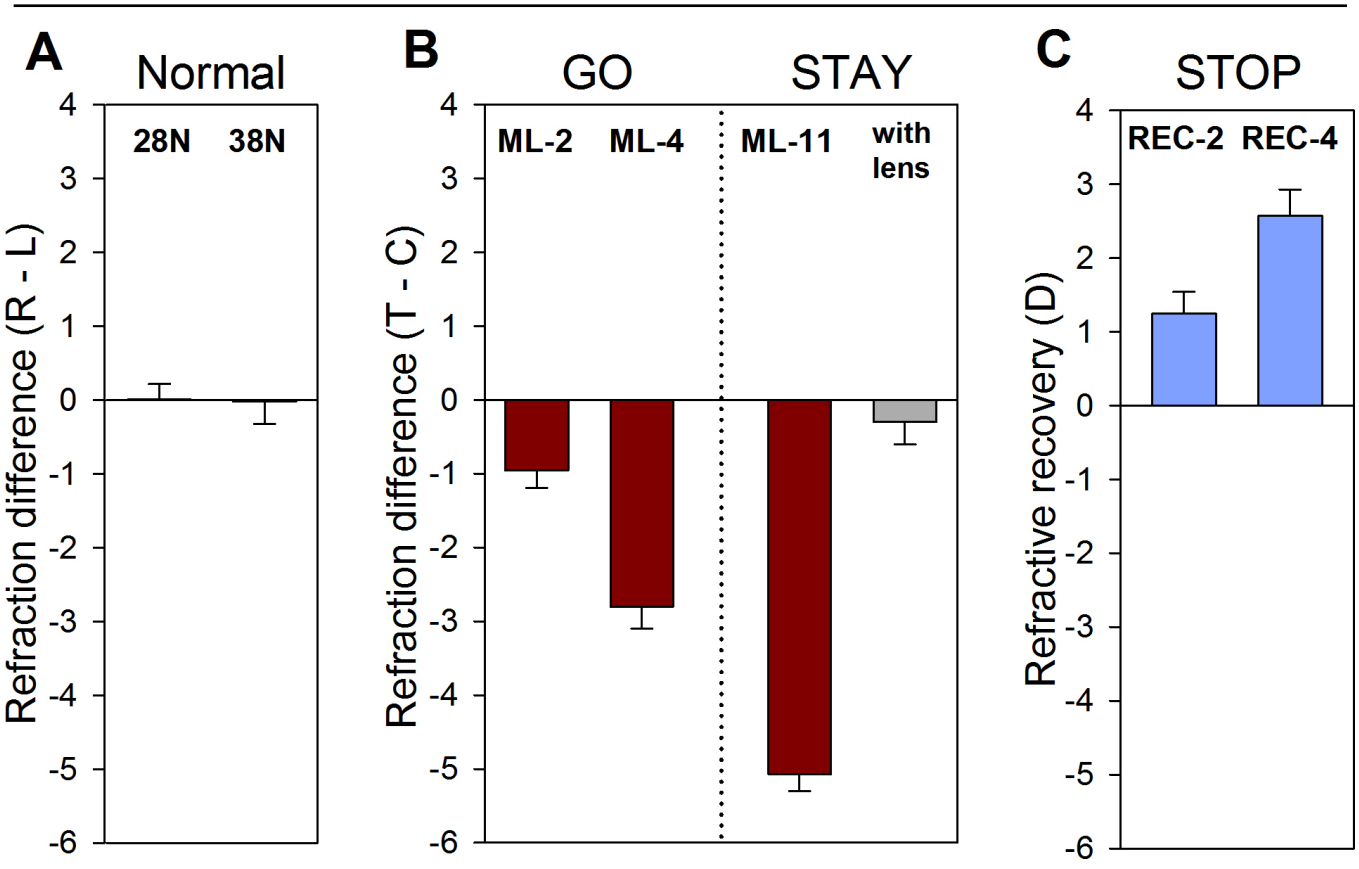

Figure 2. Refractive differences. Refractive differences of the (**A**) normal and (**B**) minus-lens wear groups. **C**: Refractive recovery from full compensation. Values are the mean refractive differences±SEM for the right – left eyes of the normal groups, and treated – control eyes for the ML and REC groups. The with-lens values in (**B**) show the treated eye – control eye difference while the –5 D lens was in place. Treated eyes in all groups were significantly myopic relative to their fellow control eyes. The upward bars in (**C**) indicate the amount of recovery (decrease in myopia) between the start and end of recovery.

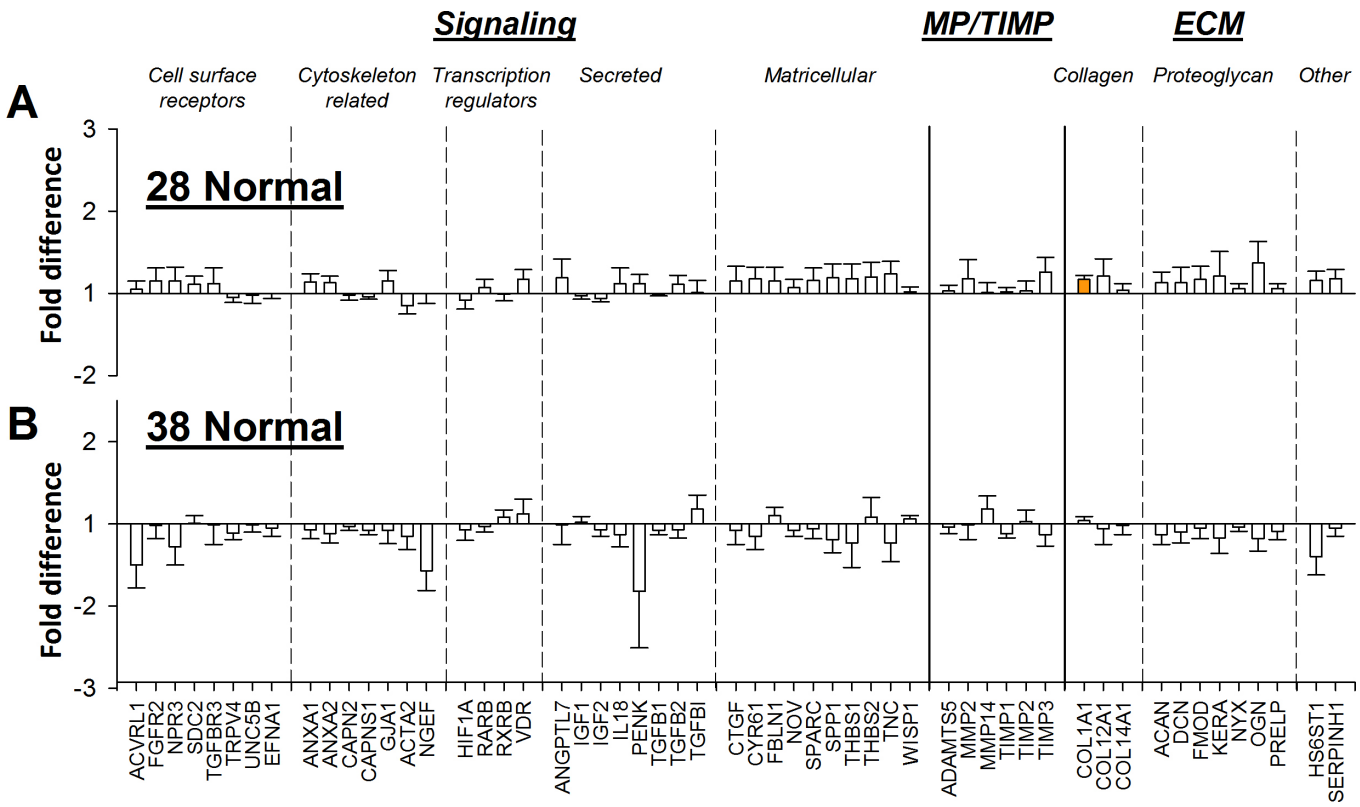

Figure 3. Gene expression differences. Comparison of gene expression fold differences in normal eyes (right versus left). **A**: 28 days of visual experience (DVE) normal group. **B**: 38 DVE normal group. Filled bars represent statistically significant differences between the right and left eyes ($p<0.05$). A positive bar indicates that expression was higher in the right eyes. Error bars=SEM. The data in panel (**A**) are reproduced with permission from [45].

variability in expression across animals within each group was low, as evidenced by the small SEM values. The GO patterns were reported previously as part of a larger study [45] and are presented here to allow comparison with the STAY and STOP expression patterns. Most but not all of the sampled genes were downregulated in the treated eyes relative to the control eyes.

It is evident in Figure 5A,B that the gene expression pattern of the ML-2 group was similar to the pattern of the ML-4 group [45]. The correlation between the fold differences in the ML-2 group versus those in the ML-4 group was high ($r^2=0.76$, $p<0.001$) with no outliers, suggesting that there was a consistent GO signature. The slope of the correlation (0.88) indicated that the signature was stronger after 4 days.

STAY: 11-day minus lens treatment: Figure 5C shows the fold differences in gene expression between the treated and control eyes in the STAY (ML-11) group; expression values are also listed in Figure 4. Three genes showed significant downregulation (*PENK*, *TGFB1*, and *ACAN*). Comparing the patterns in Figure 5B and Figure 5C, the (nonsignificant) fold differences for most of the genes in the ML-11 group were similar to those of the ML-4 group, except they were smaller and not statistically significant in this group of seven animals. This similarity is shown in Figure 6, which compares the ML-4 group GO pattern (Figure 5B) with that of the STAY (ML-11) group (Figure 5C). The correlation between the two ($r^2=0.46$) was statistically significant ($p<0.001$). The low slope (0.27) reflected the finding that the magnitude of the fold differences was smaller in the STAY group.

STOP: 2-day and 4-day recovery: As shown in Figure 5D,E, the gene expression patterns of both the REC-2 and REC-4 groups were very different from those of the GO and STAY groups and similar to each other. Few genes were downregulated (two in the REC-2 group, three in the REC-4 group) and many were upregulated (REC-2, 12; REC-4, 17). The downregulated genes included members of the signaling group (cell surface receptors and secreted signal proteins) and the extracellular matrix group (proteoglycans).The upregulated genes included ones for signaling molecules (cell surface receptors, cytoskeletal-related proteins, secreted signal proteins, and matricellular proteins), TIMPs, collagens, and proteoglycans.

	Normals		GO		STAY	STOP	
	28N	*38N*	*ML-2*	*ML-4*	*ML-11*	*REC-2*	*REC-4*
Signaling – Cell surface							
ACVRL1	1.05	-1.50	**-1.96**	-1.77	-1.27	**1.81**	**1.83**
FGFR2	1.15	-1.02	-1.59	-1.61	-1.19	1.21	1.07
NPR3	1.15	-1.28	**-7.66**	**-5.71**	-1.80	**3.42**	**4.50**
SDC2	1.11	1.01	-1.42	**-1.26**	-1.05	1.28	1.20
TGFBR3	1.12	-1.01	-1.16	1.40	-1.08	-1.79	**-1.79**
TRPV4	-1.05	-1.11	**-1.44**	-1.35	-1.13	**1.47**	**1.37**
UNC5B	-1.02	-1.01	**-1.79**	-1.84	-1.32	**1.58**	**1.51**
EFNA1	-1.00	-1.05	-1.05	-1.21	-1.09	-1.02	1.03
Signaling – Cytoskeleton related							
ANXA1	1.14	-1.07	**-1.53**	**-1.70**	-1.11	1.35	1.15
ANXA2	1.13	-1.12	**-1.94**	**-2.09**	-1.32	1.31	**1.20**
CAPN2	-1.02	-1.03	**-1.36**	-1.26	-1.11	1.18	1.16
CAPNS1	-1.04	-1.08	**-1.26**	**-1.46**	-1.02	**1.28**	**1.18**
GJA1	1.15	-1.08	-1.43	-1.38	-1.27	-1.11	-1.23
ACTA2	-1.15	-1.15	1.11	1.22	1.21	-1.18	1.02
NGEF	-1.00	-1.57	**-4.71**	**-3.95**	-1.80	**2.64**	**1.91**
Signaling – Transcription regulators							
HIF1A	-1.08	-1.07	**-1.56**	**-1.43**	-1.07	1.15	1.05
RARB	1.07	-1.03	-1.36	**-1.49**	-1.16	1.14	1.06
RXRB	-1.01	1.08	-1.21	-1.21	-1.39	1.18	-1.09
VDR	1.17	1.12	-1.43	-1.29	-1.51	1.33	1.09
Signaling – Secreted							
ANGPTL7	1.19	-1.01	-1.13	-1.06	-1.05	-1.16	-1.33
IGF1	-1.03	1.02	-1.10	1.06	1.01	-1.26	**-1.29**
IGF2	-1.06	-1.07	1.00	-1.08	1.04	-1.06	-1.01
IL18	1.12	-1.13	**-2.59**	**-3.06**	-1.50	2.09	**2.03**
PENK	1.12	-1.82	**-1.74**	**-3.67**	**-3.24**	**-2.05**	-1.01
TGFB1	-1.01	-1.08	**-1.18**	**-1.39**	**-1.16**	**1.22**	**1.23**
TGFB2	1.11	-1.07	**-2.41**	**-1.87**	-1.25	1.39	1.25
TGFBI	1.01	1.18	-1.14	**1.59**	1.06	1.03	-1.30
Signaling – Matricellular							
CTGF	1.15	-1.08	**-3.54**	**-3.02**	-1.39	**2.76**	**2.45**
CYR61	1.18	-1.15	**-2.96**	**-3.34**	-1.55	1.74	1.73
FBLN1	1.15	1.10	-1.08	**1.69**	1.32	1.64	1.16
NOV	1.07	-1.08	**-1.81**	**-1.93**	1.01	**1.58**	**1.48**
SPARC	1.16	-1.06	-1.42	**-1.43**	-1.23	1.11	1.19
SPP1	1.19	-1.19	**-1.52**	**-1.58**	1.01	1.25	1.27
THBS1	1.18	-1.23	**-2.90**	**-2.67**	-2.23	1.19	1.40
THBS2	1.20	1.08	-1.42	-1.26	-1.64	1.49	1.28
TNC	1.24	-1.23	-1.77	**-2.13**	-1.31	1.51	1.16
WISP1	1.02	1.06	-1.12	1.17	-1.04	**1.25**	**1.40**
MPs / TIMPs							
ADAMTS5	1.03	-1.04	-1.19	-1.10	-1.03	-1.26	-1.21
MMP2	1.18	-1.01	-1.26	1.16	-1.08	1.02	-1.22
MMP14	1.01	1.18	1.07	**2.11**	1.14	1.24	1.05
TIMP1	1.02	-1.12	**-1.26**	**-1.54**	-1.04	**1.20**	**1.23**
TIMP2	1.03	1.03	-1.31	-1.22	-1.54	1.07	-1.07
TIMP3	1.26	-1.13	**-2.63**	**-3.33**	-1.59	1.38	**1.75**
Extracellular matrix – Collagens							
COL1A1	**1.17**	1.04	**-1.15**	**-1.40**	-1.34	1.09	**1.48**
COL12A1	1.21	-1.06	**-2.26**	**-1.98**	-1.71	1.30	1.58
COL14A1	1.04	-1.02	-1.47	-1.05	1.02	1.10	1.28
Extracellular matrix – Proteoglycans							
ACAN	1.13	-1.13	**-2.08**	**-2.53**	**-1.42**	1.54	**1.70**
DCN	1.13	-1.10	-1.33	**-1.53**	-1.17	-1.09	-1.09
FMOD	1.17	-1.05	-1.45	**-1.73**	-1.47	1.14	1.06
KERA	1.21	-1.17	-1.49	**-1.59**	-1.03	-1.06	1.20
NYX	1.06	-1.04	-1.00	**-1.36**	-1.32	**-1.36**	**-1.29**
OGN	1.37	-1.18	**-2.00**	**-3.05**	-1.53	1.14	1.39
PRELP	1.06	-1.09	-1.17	-1.18	-1.37	-1.11	1.02
Extracellular matrix – Other							
HS6ST1	1.16	-1.40	**-1.72**	**-1.77**	-1.13	**1.96**	**2.36**
SERPINH1	1.18	-1.05	**-1.75**	**-1.69**	-1.23	1.43	1.38

Figure 4. Numerical gene expression differences. Gene expression differences comparing right vs. left eyes (Normals) or treated vs. control eyes (ML and REC). Red text indicates significant down-regulation, blue text indicates significant up-regulation and grey text indicates that the expression difference was not statistically significant (t-test, alpha = 0.05).

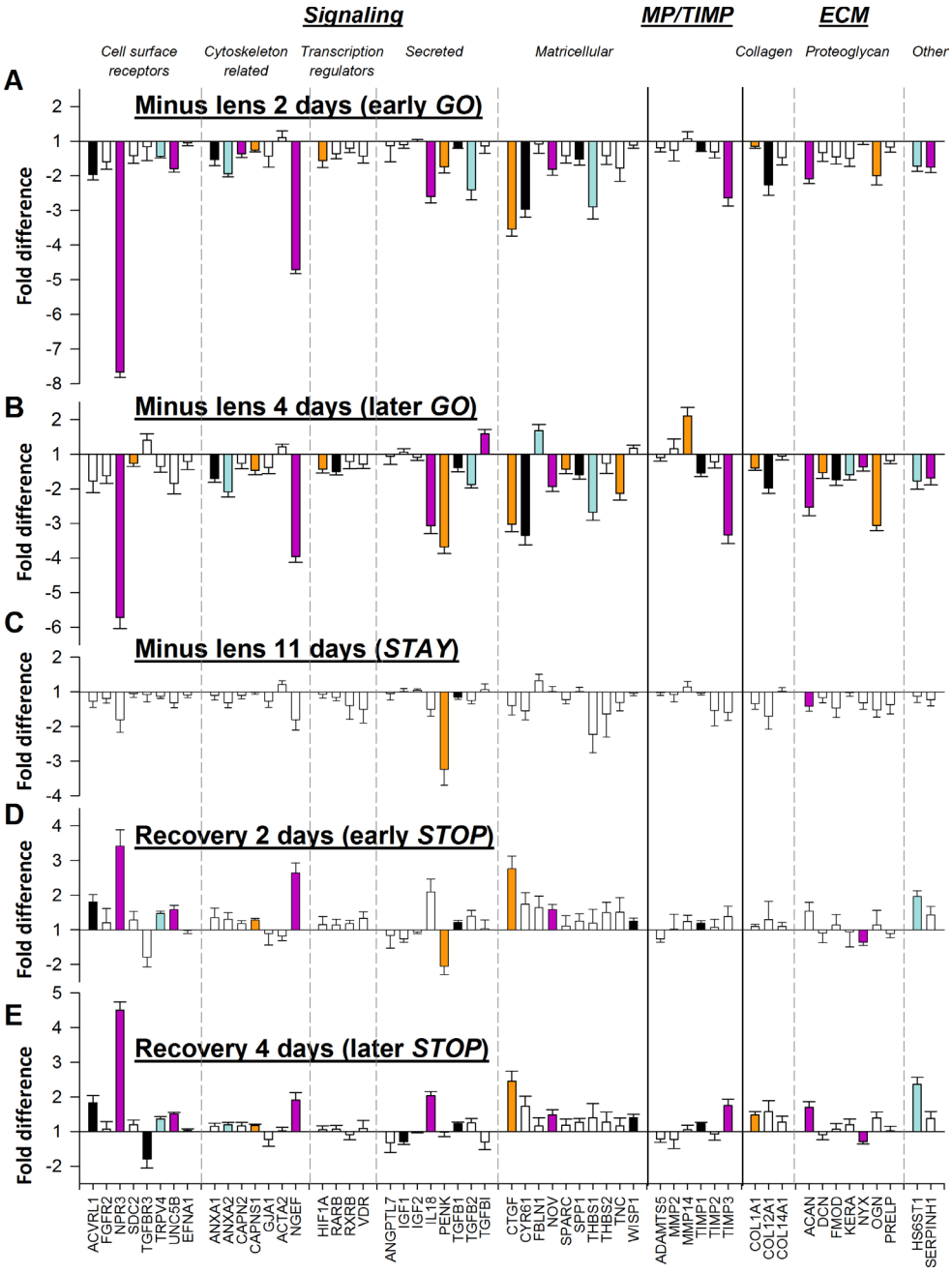

Figure 5. Gene expression differences. Comparison of gene expression differences (treated eye versus control eye) produced by (**A**) 2 days of minus-lens wear, (**B**) 4 days of minus-lens wear, (**C**) 11 days of minus-lens wear, (**D**) 2 days of recovery from 11 days of minus-lens wear, and (**E**) 4 days of recovery from 11 days of minus-lens wear. Bar color is arbitrary and intended to help in comparing the same gene in the five different conditions. Error bars=SEM. The data in panels (A) and (B) are reproduced with permission from [45] and are presented here for comparison.

The similar recovery patterns seen in Figure 5D (REC-2) and Figure 5E (REC-4) are compared in Figure 7. The gene expression patterns were highly correlated (r^2=0.76, p<0.001). The fold differences for all genes in both groups were in the same direction but differed in that fewer of the differences in the REC-2 group were statistically significant. mRNA levels of 13 genes were significantly different in both the REC-2 and REC-4 groups (Figure 8), and an additional seven genes were significant only in REC-4. One gene (*PENK*) was significantly affected in the REC-2 group but not the REC-4 group. The slope of the correlation (0.80) suggested that the overall magnitude of the fold differences in the REC-4 group was somewhat greater than in the REC-2 group.

Comparison of the GO and STOP patterns: An aim of this study was to learn how the STOP gene expression pattern differed from the GO pattern. The two GO groups and the two STOP groups are compared in Figure 9A, which compares the REC-2 pattern (Figure 5D) with the ML-2 pattern (Figure 5A); Figure 9B compares the REC-4 pattern (Figure 5E) with

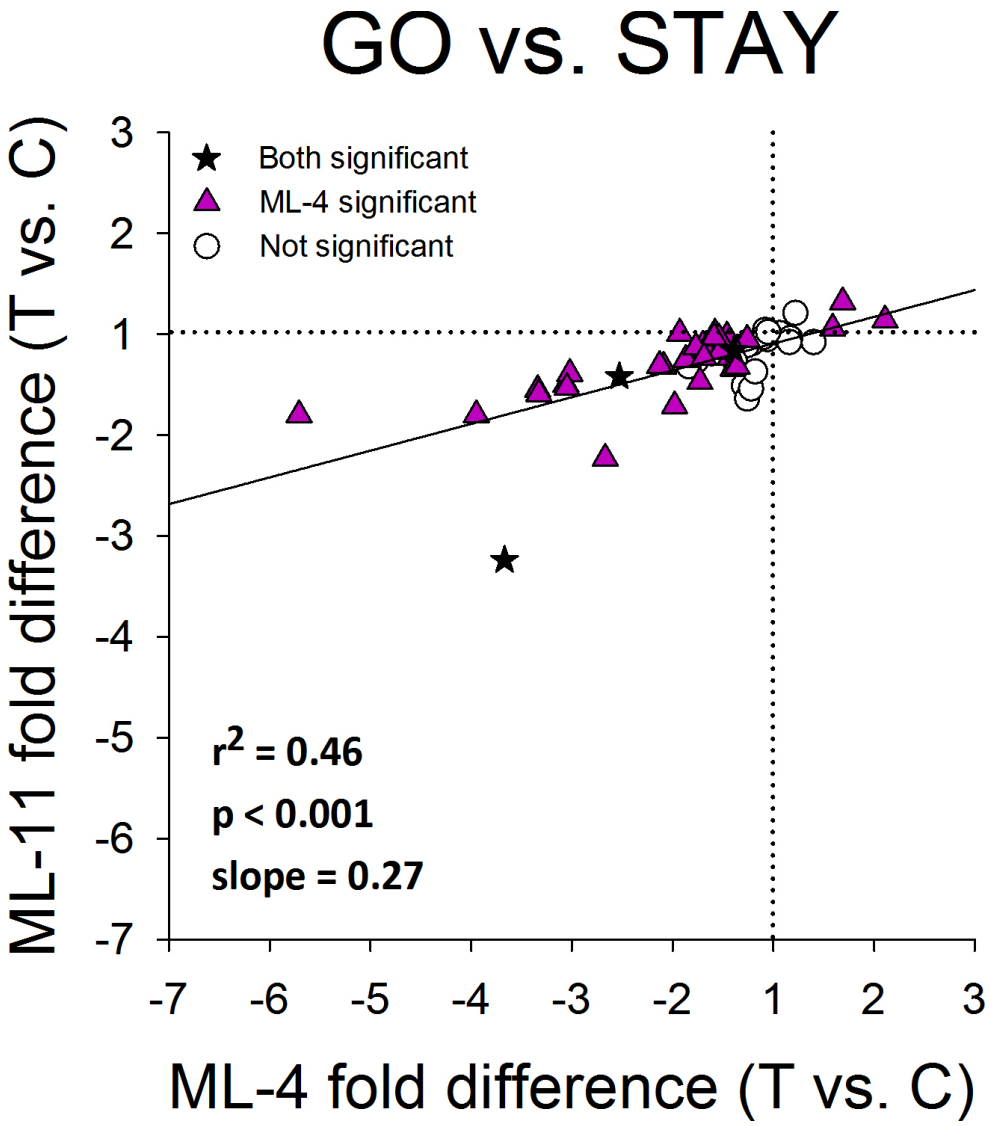

Figure 6. Gene expression differences. Comparison of the gene expression differences (treated eye versus control eye) in Figure 5C (ML-11) with the differences in Figure 5B (ML-4). The patterns of differential expression in both conditions were similar. Stars represent significant fold differences for both ML-11 and ML-4; triangles represent significant fold differences only for ML-4; circles show fold differences not significant in either treatment.

the ML-4 pattern (Figure 5B). As expected from Figure 5, the GO and STOP patterns differed from each other and differed in a similar way at both time points. The correlation between GO and STOP in each case was highly significant (2-day, $p<0.001$, $r^2=0.62$; 4-day, $p<0.001$, $r^2=0.57$) with a negative slope (−0.40 and −0.46, respectively), indicating that the STOP pattern was, in general, opposite to the GO pattern and that the overall fold-difference magnitude was lower in STOP than in GO.

At both time points, there were genes (indicated by stars) that showed significant expression differences in both GO and STOP. All were downregulated in GO and all but two (*PENK* and *NYX*) were significantly upregulated in STOP, indicating that they were bidirectionally regulated. Eleven genes were bidirectionally regulated after 2 days, and 13 genes were bidirectionally regulated after 4 days; eight of these (*NPR3*, *CAPNS1*, *NGEF*, *TGFB1*, *CTGF*, *NOV*, *TIMP1*, and *HS6ST1*) showed bidirectional regulation at both time points (Figure 8). Additional genes at both time points (triangles) showed significant expression differences in GO but not in STOP. All were downregulated after 2 days, and all but three were downregulated after 4 days. Expression of other genes (squares) was not significantly altered during GO but showed significant expression differences in STOP. There were two such genes in the 2-day GO versus STOP comparison and six in the 4-day comparison. *TGFBI*, *FBLN1*, and *MMP14* showed significant upregulation in the ML-4 group but not in the ML-2 group. *PENK* was downregulated significantly in both GO groups, in the STAY group, and in the REC-2 group but was not differentially regulated in the

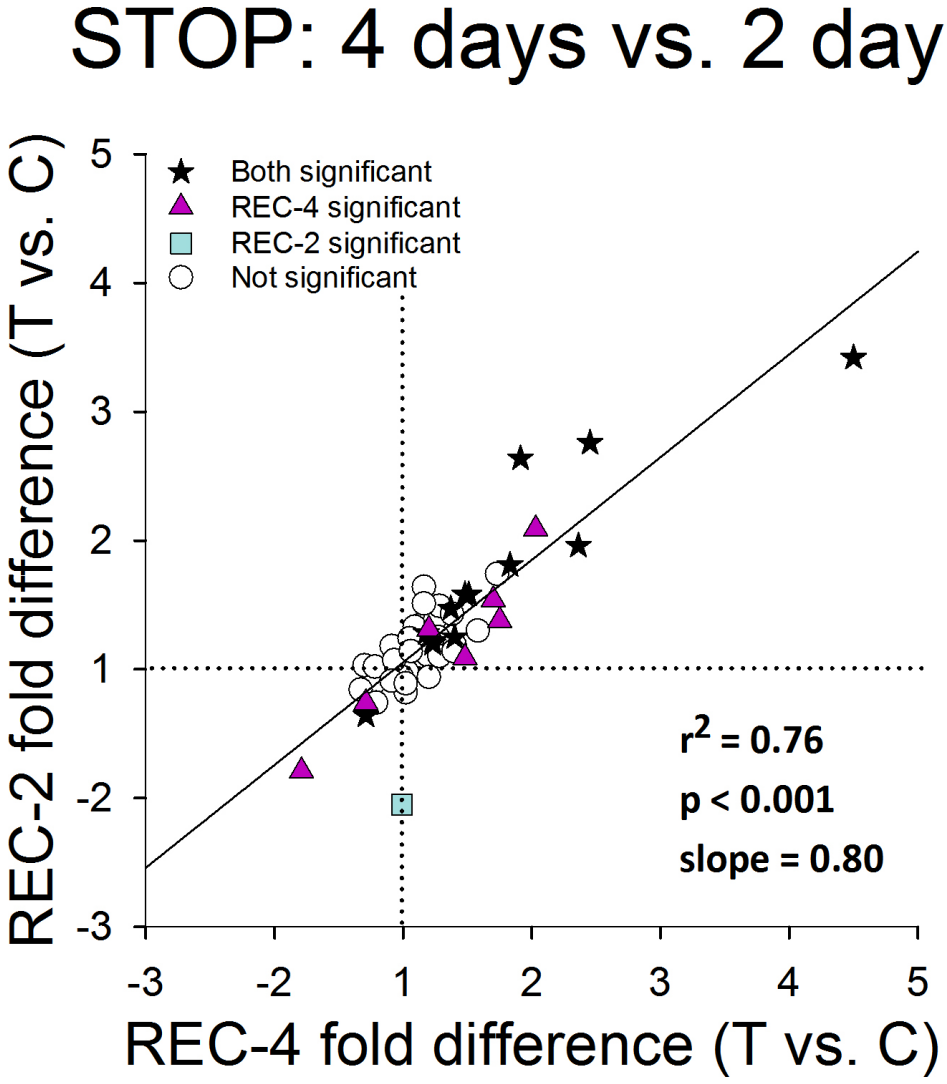

Figure 7. Gene expression differences. Comparison of the gene expression differences (treated eye [T] versus control eye [C]) in Figure 5E (REC-4) with the differences in Figure 5D (REC-2). The amount of differential expression in both conditions was similar. Stars represent significant fold differences for both REC-4 and REC-2; triangles represent significant fold differences only for REC-4; squares represent significant fold differences only for REC-2; circles show fold differences not significant in either treatment.

	Signaling					MPs / TIMPs	ECM		
	Cell surface receptors	*Cytoskeleton related*	*Transcription regulators*	*Secreted*	*Matricellular*		*Collagens*	*Proteoglycans*	*Other*
GO (ML)	***NPR3***	ANXA1 ANXA2 ***CAPNS1*** ***NGEF***	HIF1A	IL18 PENK ***TGFB1*** TGFB2	***CTGF*** CYR61 ***NOV*** SPP1 THBS1	***TIMP1*** TIMP3	COL1A1 COL12A1	ACAN OGN	***HS6ST1*** SERPINH1
STOP (REC)	ACVRL1 ***NPR3*** TRPV4 UNC5B	***CAPNS1*** ***NGEF***		***TGFB1***	***CTGF*** ***NOV*** WISP1	***TIMP1***		NYX	***HS6ST1***

Figure 8. Genes showing significant regulation at both time-points in GO and STOP. Red text indicates significant down-regulation, blue text indicates significant up-regulation, bold italic font indicates bi-directional regulation.

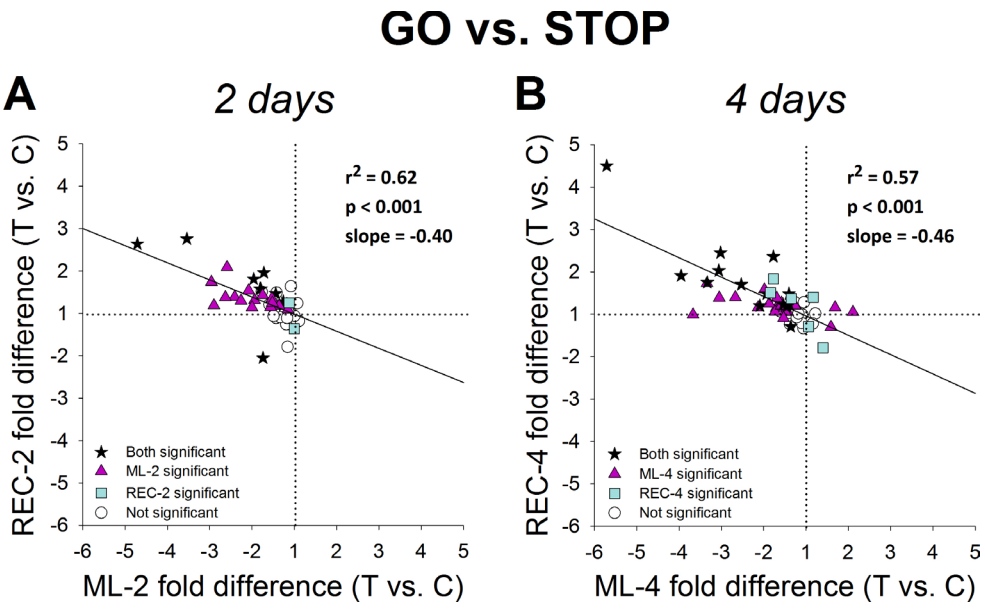

Figure 9. Comparison of treated versus control eye gene expression differences in Figure 5. Panel **A** compares the REC-2 pattern (Figure 5D) with the ML-2 pattern (Figure 5A); panel **B** compares the REC-4 pattern (Figure 5E) with the ML-4 pattern (Figure 5B). As expected from Figure 5, the GO and STOP patterns differed from each other and differed in a similar way at both time points. Stars represent significant fold differences for both treatments; triangles represent significant fold differences only for ML; squares represent significant fold differences only for REC, represent fold differences not significant for either treatment.

REC-4 group. Significant downregulation of *TGFBR3* and *IGF1* occurred in the REC-4 group but not in any other group. *NYX* was significantly downregulated after 4 days of GO and remained downregulated in both STOP groups.

Comparison with normal eyes: As in previous studies of gene expression differences during minus-lens wear and recovery, genes in the control eyes of the treated groups showed significant expression differences from the normal eyes even though, refractively, they did not differ from normal eyes. This raised the question of how the treated eye gene expression values compare with normal eye values—is the differential gene expression due mostly to a change in the treated eyes? This comparison in the two GO groups (ML-2 and ML-4) with the 28N group was reported in our previous paper [45] where we showed that the treated versus normal pattern in GO was very similar to the treated eye versus control eye pattern. When the GO versus STOP patterns at 2 days and 4 days were re-plotted using treated eye expression values compared with normal eye values (data not shown), a pattern similar to that shown in Figure 9 was found. Most of the genes whose expression was significantly downregulated relative to the control eyes in the GO condition at 2 and 4 days were also downregulated when compared with the normal eyes; during both STOP conditions, most were upregulated.

DISCUSSION

The STOP signature: Differential gene expression patterns, in which the treated eyes differ from the control eyes, are of interest because it is the treated eyes that increase their creep rate and axial elongation rate during lens compensation and decrease them during recovery, whereas they remain relatively normal in the control eyes [30,40]. The purpose of the present study was to investigate if there is a scleral fibroblast mRNA expression STOP signature for the same 55 genes examined during GO [45] and if so, to compare it with the GO signature. The sampled genes clearly show that after two days of recovery from lens-induced myopia, a time point when refractive recovery has begun (Figure 2), a STOP response pattern has developed that is similar to the response pattern found after 4 days when refractive recovery is well underway.

As shown in Figure 5 and Figure 7, the gene expression patterns in the two STOP (REC-2 and REC-4) groups were similar in terms of which genes were affected as well as the direction and relative magnitude of each gene's response. The regulation of mRNA expression was selective; there was a consistent group of genes whose expression was not significantly affected at either time point. The gene expression pattern appeared to become stronger over time. We previously found that there was little differential gene expression after 1 day of recovery [43]. After 2 days, 14 genes were differentially expressed, of which 12 were upregulated. After 4 days, all but one of the same genes were differentially expressed in the same direction and seven additional genes were differentially regulated, five of them upregulated. The expression differences for these additional genes were in the same direction after 4 days as they had been after 2 days but did not reach statistical significance at the earlier time point. This pattern of mRNA expression differences, and absence of expression differences, between the treated and control

eyes may be considered to be a STOP signature for the 55 genes that we examined. It appears that scleral fibroblast gene expression and its timing are controlled with some precision when the emmetropization mechanism calls for a slowing of the axial elongation rate.

The general pattern of mRNA upregulation is consistent with prior reports that, during recovery from induced myopia, the viscoelasticity of the sclera, measured as the creep rate, rapidly decreases. There is a small gain in scleral ECM, and many protein levels return to normal, as does hyaluronan [42,44,59,60]. Those of the genes that had been examined in previous studies of tree shrew sclera generally responded in this study as previously reported [41,43,53].

STOP versus GO gene expression signatures: The presence of both GO and STOP gene expression signatures for the 55 candidate genes used in this study allows us to compare the two to learn if gene expression in STOP is the opposite (inverse) of that in GO. Although the general pattern in GO was for downregulation of most of the genes examined and the general pattern in STOP was for upregulation, the STOP signature was not an exact inverse of the GO signature. This is reasonable; the scleral remodeling needed to reduce the creep rate and slow axial elongation during recovery need not be the opposite of that required to increase the creep rate during myopia development. As summarized with bold italic font in Figure 8 there was a subset of sampled genes whose expression in STOP (after both 2 and 4 days) was the opposite of their expression in GO—they were bidirectionally regulated. However, there were additional genes whose mRNA expression was affected only in GO and still others whose expression was affected only in STOP. Thus, there is a "core" of bidirectionally regulated genes along with many additional genes whose expression is altered in only GO or STOP but not both and others in our sample not significantly altered in either condition.

It is clear from examination of Figure 4 , Figure 5, and Figure 8 that genes belonging to many functional categories are included in the GO and/or STOP signatures. The three main categories in our sample were genes whose protein products are involved in signaling, metallopeptidases and tissue inhibitors of metallopeptidases, and the ECM. The signaling category was subdivided into genes whose protein products serve as cell surface receptors, are related to cytoskeleton and cell-cell contacts, nuclear transcription regulators, secreted signaling proteins, and matricellular proteins. The ECM category was subdivided into collagens, proteoglycans, and other proteins. As shown in Figure 8, genes whose mRNA levels were differentially affected during GO or STOP included representatives from all of these nine categories. Examples from all categories, except transcriptional regulation, showed differential expression in both STOP and GO. The eight bidirectionally regulated genes at both time points in GO and STOP were distributed across six of the categories. It is not known if the bidirectionally regulated genes are more important in producing the scleral remodeling that controls axial elongation than are genes that were affected only in GO or STOP, but they are naturally of interest because the effect on axial elongation, and on scleral viscoelasticity is opposite.

The 55 genes examined in this study presumably are a subset of a much larger group of genes that show differential expression in GO and STOP conditions. A preliminary whole-transcriptome (RNA-Seq) analysis of treated and control eyes from three of the ML-4 animals and three of the REC-4 animals suggested that perhaps almost 500 genes in ML and 400 in REC (from the nearly 15,000 genes found to be expressed in tree shrew sclera) may be up- or downregulated by at least 1.20-fold (data not shown). Thus, our sampled genes were not intended to represent the whole expression profile of GO and STAY conditions. The 55 candidate genes were selected to enable us to learn if the expression differences are different during GO and STOP and to provide strong evidence that alterations in the expression of many genes with a wide range of functions are involved. The sclera clearly is a tissue in which complex biologic processes interact; examining these changes in intact eyes in their "native" state allows us to learn more about these interactions. The GO and STAY signatures may resemble an orchestra playing a concerto. At different points in the score, some instruments play loudly, others play softly, and still others remain silent. The interaction of the notes produced by the individual instruments produces the unique orchestral sound. Although this study did not examine the protein products of these genes or whether their protein levels are altered, these genes reflect altered fibroblast responses to the emmetropization-related signals from the choroid that are involved in regulating axial elongation of the sclera.

A STAY signature: As noted in Figure 2, after 11 days of minus-lens wear, the refractive hyperopia initially produced by the lens at the start of lens wear had dissipated; the refractions of the treated eyes, while wearing the −5 D lens were similar to the refractions of the control eyes. Yet, from studies in other groups of tree shrews, we assume that the axial length of the treated eyes continued to be elongated, keeping the retina located at the shifted focal plane [30,40,42]. That something (the STAY signal) actively maintained the with-the-lens emmetropia is demonstrated by the rapid recovery that developed soon after minus-lens wear is stopped. If the GO condition is one of an accelerated axial elongation

rate and STOP one where the elongation rate decelerated, then STAY is a condition of maintained axial elongation rate. A STAY signal would be analogous to the pressure on the accelerator pedal of a car needed to maintain highway speed. Clear evidence for a STAY signature in the choroid was found in a previous study of mRNA expression from this laboratory [36]. This led us to examine the gene expression pattern in the ML-11 group to learn if there was evidence for a STAY signature in the responses of the scleral fibroblasts. Although our prior study that examined fewer genes did not find significant regulation of gene expression after 11 days of minus lens wear [43], our expanded sample of genes found three (*PENK*, *TGFB1*, and *ACAN*) that showed statistically significant differential expression in the ML-11 group. These three also showed significant differential regulation in the same direction (downregulation) in both the ML-2 and ML-4 groups. Significant expression of these few genes would not seem to constitute a "signature". However, when comparing the differential expression of all 55 genes at ML-11 and ML-4 (Figure 6), we noted that there were also small differences in the expression of numerous other genes that were significantly affected in ML-4 but whose expression did not reach statistical significance at ML-11. These nonsignificant fold differences included 29 genes regulated in the same direction (26 downregulated) as they were at ML-4 when the differences were statistically significant. Only two genes did not follow this pattern. Whether or not to give weight to these consistent but nonsignificant differences is an issue of interest considering the relatively low statistical power that can be achieved with groups of seven animals. We suggest here that there may be evidence of a STAY signature in the sclera. If so, it appears to be weaker than the choroidal STAY signature.

Summary: This study examined differential mRNA expression by mammalian scleral fibroblasts during refractive recovery from lens-induced myopia, a STOP condition, and compared it with expression of the same genes during minus-lens wear, a GO condition, and after the completion of minus-lens compensation, a STAY condition. Based on this sample of 55 genes, we found that the scleral fibroblasts respond with distinctly different mRNA expression signatures to the different emmetropization conditions. The signature for this sample of genes is mostly, but not entirely, upregulation in the STOP condition in contrast with the mostly downregulation in the GO and STAY conditions. In both GO and STOP, the 4-day time points showed stronger alterations in gene expression level and a greater number of significantly affected genes than the 2-day treatment. This corresponds to the times at which the eye's refractions are also changing most rapidly. We also found evidence in sclera for the presence of a STAY response in eyes that had completed compensation for a minus lens. The STAY signature appeared as a weakened form of the GO signature, and both were very distinct from the STOP signature. The many genes in our sample whose expression is altered suggest that the emmetropization-related responses in sclera are complex and unlikely to depend on the regulation of a single gene or even a small number of genes

APPENDIX 1. PRIMERS USED: SEQUENCES, AMPLICON SIZES, AND EFFICIENCIES.

To access the data, click or select the words "Appendix 1."

ACKNOWLEDGMENTS

This study was supported by NIH grants R01EY005922 and P30EY003039. This work was performed in partial fulfillment of the requirements for the degree of Doctor of Philosophy at the University of Alabama at Birmingham (L. Guo). Preliminary results were presented in abstract form (Guo L, et al. IOVS 2011; 52: ARVO E-Abstract 6299). None of the authors have any commercial interests in the subject of the research.

REFERENCES

1. Vitale S, Sperduto RD, Ferris FL III. Increased prevalence of myopia in the United States between 1971–1972 and 1999–2004. Arch Ophthalmol 2009; 127:1632-9. [PMID: 20008719].
2. Sperduto RD, Seigel D, Roberts J, Rowland M. Prevalence of myopia in the United States. Arch Ophthalmol 1983; 101:405-7. [PMID: 6830491].
3. Fledelius HC. Myopia prevalence in Scandinavia. A survey, with emphasis on factors of relevance for epidemiological refraction studies in general. Acta Ophthalmol Suppl 1988; 185:44-50. [PMID: 2853539].
4. Wang Q, Klein BE, Klein R, Moss SE. Refractive status in the Beaver Dam Eye Study. Invest Ophthalmol Vis Sci 1994; 35:4344-7. [PMID: 8002254].
5. Attebo K, Ivers RQ, Mitchell P. Refractive errors in an older population: The Blue Mountains Eye Study. Ophthalmology 1999; 106:1066-72. [PMID: 10366072].
6. Wensor M, McCarty CA, Taylor HR. Prevalence and risk factors of myopia in Victoria, Australia. Arch Ophthalmol 1999; 117:658-63. [PMID: 10326965].
7. Goh WSH, Lam CSY. Changes in refractive trends and optical components of Hong Kong Chinese aged 19–39 years. Ophthalmic Physiol Opt 1994; 14:378-82. [PMID: 7845695].
8. Lin LL, Shih YF, Tsai CB, Chen CJ, Lee LA, Hung PT, Hou PK. Epidemiologic study of ocular refraction among school-children in Taiwan in 1995. Optom Vis Sci 1999; 76:275-81. [PMID: 10375241].

9. Lu B, Congdon N, Liu X, Choi K, Lam DS, Zhang M, Zheng M, Zhou Z, Li L, Liu X, Sharma A, Song Y. Associations between near work, outdoor activity, and myopia among adolescent students in rural China: the Xichang Pediatric Refractive Error Study report no. 2. Arch Ophthalmol 2009; 127:769-75. [PMID: 19506196].
10. Quek TP, Chua CG, Chong CS, Chong JH, Hey HW, Lee J, Lim YF, Saw SM. Prevalence of refractive errors in teenage high school students in Singapore. Ophthalmic Physiol Opt 2004; 24:47-55. [PMID: 14687201].
11. Jung SK, Lee JH, Kakizaki H, Jee D. Prevalence of myopia and its association with body stature and educational level in 19-year-old male conscripts in Seoul, South Korea. Invest Ophthalmol Vis Sci 2012; 53:5579-83. [PMID: 22836765].
12. He M, Zeng J, Liu Y, Xu J, Pokharel GP, Ellwein LB. Refractive error and visual impairment in urban children in southern china. Invest Ophthalmol Vis Sci 2004; 45:793-9. [PMID: 14985292].
13. Lim R, Mitchell P, Cumming RG. Refractive associations with cataract: The Blue Mountains Eye Study. Invest Ophthalmol Vis Sci 1999; 40:3021-6. [PMID: 10549667].
14. Burton TC. The influence of refractive error and lattice degeneration on the incidence of retinal detachment. Trans Am Ophthalmol Soc 1989; 87:143-55. [PMID: 2562517].
15. Avila MP, Weiter JJ, Jalkh AE, Trempe CL, Pruett RC, Schepens CL. Natural history of choroidal neovascularization in degenerative myopia. Ophthalmol 1984; 91:1573-81. [PMID: 6084222].
16. Saw SM, Gazzard G, Shih-Yen EC, Chua WH. Myopia and associated pathological complications. Ophthalmic Physiol Opt 2005; 25:381-91. [PMID: 16101943].
17. Foster PJ, Jiang Y. Epidemiology of myopia. Eye (Lond) 2014; 28:202-8. [PMID: 24406412].
18. Bourne RR, Stevens GA, White RA, Smith JL, Flaxman SR, Price H, Jonas JB, Keeffe J, Leasher J, Naidoo K, Pesudovs K, Resnikoff S, Taylor HR. Causes of vision loss worldwide, 1990–2010: a systematic analysis. Lancet Glob Health 2013; 1:e339-49. [PMID: 25104599].
19. Howland HC, Waite S, Peck L. Early focusing history predicts later refractive state: a longitudinal photorefractive study. Optical Society of America 1993; 3:210-3. .
20. Gwiazda J, Thorn F, Bauer J, Held R. Emmetropization and the progression of manifest refraction in children followed from infancy to puberty. Clin Vis Sci 1993; 8:337-44. .
21. Mutti DO, Mitchell GL, Jones LA, Friedman NE, Frane SL, Lin WK, Moeschberger ML, Zadnik K. Axial growth and changes in lenticular and corneal power during emmetropization in infants. Invest Ophthalmol Vis Sci 2005; 46:3074-80. [PMID: 16123404].
22. Wallman J, Winawer J. Homeostasis of eye growth and the question of myopia. Neuron 2004; 43:447-68. [PMID: 15312645].
23. Norton TT. Animal models of myopia: Learning how vision controls the size of the eye. ILAR J 1999; 40:59-77. [PMID: 11304585].
24. Shen W, Sivak JG. Eyes of a lower vertebrate are susceptible to the visual environment. Invest Ophthalmol Vis Sci 2007; 48:4829-37. [PMID: 17898310].
25. Schaeffel F, Howland HC. Mathematical model of emmetropization in the chicken. J Opt Soc Am 1988; 5:2080-6. [PMID: 3230476].
26. Schaeffel F, Glasser A, Howland HC. Accommodation, refractive error and eye growth in chickens. Vision Res 1988; 28:639-57. [PMID: 3195068].
27. Howlett MH, McFadden SA. Emmetropization and schematic eye models in developing pigmented guinea pigs. Vision Res 2007; 47:1178-90. [PMID: 17360016].
28. Smith EL III, Hung LF, Harwerth RS. Developmental visual system anomalies and the limits of emmetropization. Ophthalmic Physiol Opt 1999; 19:90-102. [PMID: 10615445].
29. Troilo D, Nickla DL, Wildsoet CF. Form deprivation myopia in mature common marmosets (*Callithrix jacchus*). Invest Ophthalmol Vis Sci 2000; 41:2043-9. [PMID: 10892841].
30. Norton TT, Amedo AO, Siegwart JT Jr. The effect of age on compensation for a negative lens and recovery from lens-induced myopia in tree shrews (*Tupaia glis belangeri*). Vision Res 2010; 50:564-76. [PMID: 20045711].
31. Wildsoet CF. Active emmetropization - evidence for its existence and ramifications for clinical practice. Ophthalmic Physiol Opt 1997; 17:279-90. [PMID: 9390372].
32. Rohrer B, Stell WK. Basic fibroblast growth factor (bFGF) and transforming growth factor beta (TGF-β) act as stop and go signals to modulate postnatal ocular growth in the chick. Exp Eye Res 1994; 58:553-61. [PMID: 7925692].
33. Schaeffel F, Howland HC. Properties of the feedback loops controlling eye growth and refractive state in the chicken. Vision Res 1991; 31:717-34. [PMID: 1843772].
34. Irving EL, Callender MG, Sivak JG. Inducing myopia, hyperopia, and astigmatism in chicks. Optom Vis Sci 1991; 68:364-8. [PMID: 1852398].
35. Irving EL, Callender MG, Sivak JG. Inducing ametropias in hatchling chicks by defocus–aperture effects and cylindrical lenses. Vision Res 1995; 35:1165-74. [PMID: 7610578].
36. He L, Frost MR, Siegwart JT Jr, Norton TT. Gene expression signatures in tree shrew choroid during lens-induced myopia and recovery. Exp Eye Res 2014; 123:56-71. [PMID: 24742494].
37. Amedo AO, Norton TT. Visual guidance of recovery from lens-induced myopia in tree shrews (*Tupaia glis belangeri*). Ophthalmic Physiol Opt 2012; 32:89-99. [PMID: 22035177].
38. Moses RA, Grodzki WJ, Starcher BC, Galione MJ. Elastin content of the scleral spur, trabecular mesh, and sclera. Invest Ophthalmol Vis Sci 1978; 17:817-8. [PMID: 681140].

39. Rada JA, Achen VR, Perry CA, Fox PW. Proteoglycans in the human sclera: Evidence for the presence of aggrecan. Invest Ophthalmol Vis Sci 1997; 38:1740-51. [PMID: 9286262].

40. Siegwart JT Jr, Norton TT. Regulation of the mechanical properties of tree shrew sclera by the visual environment. Vision Res 1999; 39:387-407. [PMID: 10326144].

41. Siegwart JT Jr, Norton TT. Selective regulation of MMP and TIMP mRNA levels in tree shrew sclera during minus lens compensation and recovery. Invest Ophthalmol Vis Sci 2005; 46:3484-92. [PMID: 16186323].

42. Moring AG, Baker JR, Norton TT. Modulation of glycosaminoglycan levels in tree shrew sclera during lens-induced myopia development and recovery. Invest Ophthalmol Vis Sci 2007; 48:2947-56. [PMID: 17591859].

43. Gao H, Frost MR, Siegwart JT Jr, Norton TT. Patterns of mRNA and protein expression during minus-lens compensation and recovery in tree shrew sclera. Mol Vis 2011; 17:903-19. [PMID: 21541268].

44. Frost MR, Norton TT. Alterations in protein expression in tree shrew sclera during development of lens-induced myopia and recovery. Invest Ophthalmol Vis Sci 2012; 53:322-36. [PMID: 22039233].

45. Guo L, Frost MR, He L, Siegwart JT Jr, Norton TT. Gene expression signatures in tree shrew sclera in response to three myopiagenic conditions. Invest Ophthalmol Vis Sci 2013; 54:6806-19. [PMID: 24045991].

46. Siegwart JT, Norton TT. Goggles for controlling the visual environment of small animals. Lab Anim Sci 1994; 44:292-4. [PMID: 7933981].

47. Norton TT, Wu WW, Siegwart JT Jr. Refractive state of tree shrew eyes measured with cortical visual evoked potentials. Optom Vis Sci 2003; 80:623-31. [PMID: 14502042].

48. McKanna JA, Casagrande VA. Atropine affects lid-suture myopia development. Doc Ophthalmol Proc Ser 1981; 28:187-92. .

49. Norton TT, Siegwart JT Jr, Amedo AO. Effectiveness of hyperopic defocus, minimal defocus, or myopic defocus in competition with a myopiagenic stimulus in tree shrew eyes. Invest Ophthalmol Vis Sci 2006; 47:4687-99. [PMID: 17065475].

50. Norton TT, Siegwart JT, German AJ, Robertson J, Wu WW. Comparison of cycloplegic streak retinoscopy with autorefractor measures in tree shrew eyes with, and without, induced myopia. ARVO Annual Meeting; 2000 April 30-May 5; Fort Lauderdale (FL).

51. Glickstein M, Millodot M. Retinoscopy and eye size. Science 1970; 168:605-6. [PMID: 5436596].

52. Norton TT, McBrien NA. Normal development of refractive state and ocular component dimensions in the tree shrew (*Tupaia belangeri*). Vision Res 1992; 32:833-42. [PMID: 1604852].

53. He L, Frost MR, Siegwart JT Jr, Norton TT. Adhesion-related protein and vitamin D receptor mRNA levels in tree shrew sclera during minus lens treatment and during recovery. ARVO Annual Meeting; 2010 May 2–6; Fort Lauderdale (FL).

54. Siegwart JT Jr, Strang CE. Selective modulation of scleral proteoglycan mRNA levels during minus lens compensation and recovery. Mol Vis 2007; 13:1878-86. [PMID: 17960126].

55. Livak KJ, Schmittgen TD. Analysis of relative gene expression data using real-time quantitative PCR and the $2^{-\Delta\Delta Ct}$ method. Methods 2001; 25:402-8. [PMID: 11846609].

56. McBrien NA, Norton TT. The development of experimental myopia and ocular component dimensions in monocularly lid-sutured tree shrews (*Tupaia belangeri*). Vision Res 1992; 32:843-52. [PMID: 1604853].

57. Shaikh AW, Siegwart JT, Norton TT. Effect of interrupted lens wear on compensation for a minus lens in tree shrews. Optom Vis Sci 1999; 76:308-15. [PMID: 10375247].

58. Norton TT, Rada JA. Reduced extracellular matrix accumulation in mammalian sclera with induced myopia. Vision Res 1995; 35:1271-81. [PMID: 7610587].

59. Gentle A, Liu Y, Martin JE, Conti GL, McBrien NA. Collagen gene expression and the altered accumulation of scleral collagen during the development of high myopia. J Biol Chem 2003; 278:16587-94. [PMID: 12606541].

60. McBrien NA, Jobling AI, Gentle A. Biomechanics of the sclera in myopia: extracellular and cellular factors. Optom Vis Sci 2009; 86:E23-30. [PMID: 19104466].

Articles are provided courtesy of Emory University and the Zhongshan Ophthalmic Center, Sun Yat-sen University, P.R. China. The print version of this article was created on 9 December 2014. This reflects all typographical corrections and errata to the article through that date. Details of any changes may be found in the online version of the article.